Separation Science and Technology
Publication details, including instructions for authors and subscription information:
http://www.informaworld.com/smpp/title~content=t713708471

Mass transfer properties of monoliths

R. Hahn[a]; M. Panzer[b]; E. Hansen[c]; J. Mollerup[c]; A. Jungbauer[a]
[a] Institute for Applied Microbiology, University of Agricultural Sciences, Vienna, Austria [b] Department of Chemical Engineering, University of Delaware, Newark, DE, U.S.A. [c] Engineering Research Center IVC-SEP, Department of Chemical Engineering, Technical University of Denmark, Lyngby, Denmark

Online publication date: 29 May 2002

SEPARATION SCIENCE AND TECHNOLOGY, 37(7), 1545–1565 (2002)

MASS TRANSFER PROPERTIES OF MONOLITHS

R. Hahn,[1] M. Panzer,[2] E. Hansen,[3] J. Mollerup,[3] and A. Jungbauer[1,*]

[1]Institute for Applied Microbiology, University of Agricultural Sciences, Muthgasse 18, A-1190, Vienna, Austria
[2]Department of Chemical Engineering, University of Delaware, Newark, DE 19716
[3]Engineering Research Center IVC-SEP, Department of Chemical Engineering, Technical University of Denmark, DTU, Building 229, 2800 Lyngby, Denmark

ABSTRACT

The mass transfer properties of polyglycidylmethacrylate–ethylenedimethacrylate monolithic ion-exchangers (convective interaction media disks) were evaluated. As a reference material, the particulate ion-exchanger Source 30 was selected. The model proteins lysozyme, bovine serum albumin, and IgG were loaded at different concentrations and velocities. The mass transfer zones obtained with the monoliths were affected by neither the linear flow velocity nor the protein concentration in the mobile phase. The reduced height equivalent to one theoretical plate (HETP) of monoliths were independent of the reduced velocity. This was not the case for the particulate material.

*Corresponding author. Fax: 43 1 3697615; E-mail: jungbaue@hp01.boku.ac.at

Key Words: Proteins; Monoliths; Ion-exchanger; Two-film model; Mass transfer

INTRODUCTION

Monolithic columns specially designed for the fast separation of biopolymers such as proteins and polynucleotides have been developed using organic polymers or inorganic material (1–3). In contrast to conventional media, the chromatography gel is polymerized directly into the chromatography column and a three-dimensional network is formed. Scanning electron micrograph pictures of monoliths show a latticelike structure with a high connectivity or agglomerates of small particles (4–6). Common to these monoliths is their high porosity; as a consequence, the pressure drop is low (7). In the past, many reports have demonstrated the benefits of monoliths for the fast separation of proteins and polynucleotides as reviewed by Josic and Strancar (8) and Josic et al. (9).

It has been hypothesized that the high efficiency of monoliths is due to enhanced mass transfer explained by increased convective transport of the solutes. According to the structure of the monolith, the solute transport into the bed is by convection, while transport into the pores is by diffusion—similar to what is observed in particulate chromatography resins. So far, the mass transfer properties of monolithic columns have not been studied extensively.

A model has been developed using the cubic-lattice model to describe the breakthrough behavior of monoliths (10). Iberer et al. (11), Garke et al. (12), and Liao (5) showed that within a certain velocity range, the shape of the breakthrough curves (BTCs) do not change. This indicates a very fast mass transfer and allows the speculation that the mass transfer is not dominated by the chromatographic velocity.

Yoshida et al. (13) proposed a theoretical solution to extract the film and intraparticle resistances from BTCs for adsorption on ion-exchange systems with irreversible equilibrium. They have correlated experimental data for the ion-exchange of inorganic salts and for the adsorption of moisture with this model. Fernandez et al. (14) have applied this model for adsorption of proteins on ion-exchangers specially designed for protein chromatography. Hansen and Mollerup (15) developed a two-film model for simultaneous determination of the external and the solid-phase mass transfer coefficients.

Monolithic columns based on polyglycidylmethacrylate–ethylenedimethacrylate as developed by Tennikova et al. (2) have a very similar structure to conventional packed beds with the special feature of extremely small particles

and a very high porosity, as shown by Hahn and Jungbauer (4). During the polymerization, small particles agglomerate to a homogeneous medium. The interstitial space is formed by precipitation of the formed polymer, since solubility decreases with growth of the chains in length. After polymerization, the solvent is washed out. The expansion of this space in determined by the composition of the solvents, the so-called porogenes. This open space can be reached by convective flow, whereas the pores in the small particles are reached only by diffusion.

Therefore it is obvious to treat monoliths based on macroporous polyglycidylmethacrylate–ethylenedimethacrylate in a similar way as a conventional packed bed. We have selected Source ion-exchangers as the reference material for a particulate sorbent. Convective interaction media disks (CIM-disks) and Source were fed with various model proteins with different sizes at various feed concentrations and velocities and mass transfer coefficients were derived from the BTCs.

THEORY

The shape of the BTCs is determined by the equilibrium isotherm, by mass transfer resistances, and by the axial dispersion.

Since the flow pattern can be represented as axially dispersed plug flow the differential fluid phase mass balance is

$$-D_{\mathrm{L}}\frac{\partial^2 c}{\partial z^2}+u\frac{\partial c}{\partial z}+\frac{\partial c}{\partial t}+\left(\frac{1-\epsilon}{\epsilon}\right)\frac{\partial q}{\partial t}=0 \tag{1}$$

with D_{L} the axial dispersion coefficient, q the sorbate concentration averaged over the particle, c the fluid phase concentration, z the column length, u the interstitial fluid velocity, t the time, and ϵ the voidage of the adsorbent bed.

The mass balance for an adsorbent particle yields the adsorption rate expression, which may be written as

$$\frac{\partial q}{\partial t}=f(q,c) \tag{2}$$

This equation was either solved by assuming the overall mobile phase driving force model, the apparent overall solid-phase driving force model, or the two-film model (15). The mass balance for the adsorbate particle can be described by the apparent overall mobile phase driving force model

$$\frac{\partial q}{\partial t}=\frac{6}{d_{\mathrm{p}}}K_c(c-c^*) \tag{3}$$

or the apparent overall solid-phase driving force model

$$\frac{\partial q}{\partial t} = \frac{6}{d_p} K_q (q^* - q) \tag{4}$$

where c^* is a hypothetical mobile phase concentration in equilibrium with q, and q^* is a hypothetical solid-phase concentration in equilibrium with c. K_c and K_q are the respective apparent overall mass-transfer coefficients, and $6/d_p$ is the surface to volume ratio for spherical particles. The apparent overall driving forces are $(c - c^*)$ and $(q^* - q)$, respectively.

In the two-film theory, the linear driving forces are $(c - c_0)$ and $(q_0 - q)$ where subscript 0 denotes a concentration at the interface of the two films at which c_0 and q_0 per definition are in equilibrium, that is

$$\frac{\partial q}{\partial t} = \frac{6}{d_p} k_f (c - c_0) = \frac{6}{d_p} k_s (q_0 - q) \tag{5}$$

In this work k_f is a velocity-dependent external mass-transfer coefficient and k_s is the solid-phase mass transfer coefficient. $1/k_f$ and $1/k_s$ are termed the external and solid-phase resistances.

For certain limiting forms of the isotherm, such as linear or rectangular, and neglecting axial dispersion, analytic expressions for the BTC can be found. Vermeulen (16), for example, has demonstrated that for favorable monovalent ion-exchange or adsorption systems, BTCs can be adequately predicted by assuming that the equilibrium isotherm is rectangular when the true equilibrium constant is greater than five.

Here we follow the approach described by Hansen and Mollerup (15).

At constant pattern the mobile and solid-phase concentrations are related by Eq. (6).

$$\frac{q}{q_F} = \frac{c}{c_F} \tag{6}$$

where c_F is the feed concentration and q_F the corresponding equilibrium concentration. For constant pattern conditions, the flux equations become ordinary differential equations. It is convenient to introduce the dimensionless concentrations $x = c/c_F$ and $y = q/q_F$, therefore the constant pattern relation, Eq. (6), becomes $y = x$. Inserting Eq. (6) into the Eqs. (3) and (4) and calculating c^* and q^* from the Langmuir expression, the flux can be expressed as a function of x

$$\frac{dq}{dt} = q_F \frac{dx}{dt} = \frac{6}{d_p} K_c c_F \frac{\beta x (1 - x)}{1 + \beta (1 - x)} \tag{7}$$

and

$$\frac{dq}{dt} = q_F \frac{dx}{dt} = \frac{6}{d_p} K_q q_F \frac{\beta x(1-x)}{1+\beta x} \tag{8}$$

where $\beta = bc_F$.

Inserting the Langmuir expression and the constant pattern relation in the two-film model, Eq. (5), yields

$$\delta(x - x_0) = \frac{(1+\beta)x_0}{1+\beta x_0} - x \tag{9}$$

where δ is the scaled mass-transfer resistance ratio

$$\delta = \frac{k_f c_F}{k_s q_F} \tag{10}$$

The dimensionless interfacial mobile phase concentration x_0 is obtained by solving Eq. (9), which in the present case can be solved analytically. The flux in the two-film model is expressed as a function of x by solving Eq. (9) for x_0 and inserting in Eq. (5). The solution is

$$\frac{dq}{dt} = q_F \frac{dx}{dt} = \frac{6}{d_p} k_f c_F (x - x_0) \tag{11}$$

where

$$x_0 = D(x) + \sqrt{[D(x)]^2 + \frac{x(1+\delta)}{\delta\beta}} \tag{12}$$

with

$$D(x) = \frac{1}{2}\left(x + \frac{x}{\delta} - \frac{1}{\beta} - \frac{1}{\delta} - \frac{1}{\delta\beta}\right). \tag{13}$$

MATERIALS AND METHODS

The model compounds lysozyme and bovine serum albumin (BSA) and the chemicals for buffer preparation were purchased from Sigma Aldrich (Vienna, Austria). Polyclonal human IgG was a gift from Octapharma Pharmazeutische Produktionsgesellschaft m.b.H. (Vienna, Austria). Source 30

S and Q were provided by Amersham Pharmacia Biotech (Uppsala, Sweden), CIM disks SO_3 and diethyl amino ethyl (DEAE) from BIA Separation (Ljubljana, Slovenia). The Source media were packed into HR 10 columns (inner diameter 1.0 cm) from Amersham Pharmacia Biotech. The column height was 1 cm. The CIM disks (diameter 1.2 cm, height 0.3 cm) were mounted in special cartridges. All chromatography runs were performed on an ÄKTA system (Amersham Pharmacia Biotech) at room temperature. The linear velocity range was 100–800 cm/hr.

Running buffers were 20 m*M* Tris/HCl, pH 8.0 for lysozyme and BSA, and 20 m*M* sodium acetate, pH 4.5 for IgG. The proteins were applied in a concentration range of 0.1–3.0 mg/mL until breakthrough was achieved. Elution was carried out with 2 *M* NaCl, dissolved in the corresponding running buffer. After each run, the sorbents were immediately regenerated by applying 2 mL of 1 *M* NaOH.

RESULTS AND DISCUSSION

The objective of the work was to study of the mass transport properties of monoliths. A polyglycidylmethacrylate–ethylenedimethacrylate monolith from BIA Separations was used as a model. For comparison, the ion-exchange media Source 30 Q and S from Amersham Pharmacia Biotech were used. The diameter of these monosized particles is 30 μm. This is a high performance chromatography resin used for preparative and industrial application of bioseparation.

From previous experiments we already knew that this type of monolith is constituted from very small particles with an approximate diameter of 1 μm (4). The difference from conventional media is that interparticle bonds are stabilizing the bed. From these observations, it might be possible to treat the mass transport of monoliths analogously to conventional media. The monolith is also used for preparative purposes (17). Therefore it was decided to compare the monolithic media with media intended for the same application.

We have selected the two-film model described by Hansen and Mollerup (15) to extract mass transfer coefficients. They showed that the model is suited for ion-exchange of proteins. A requirement of this model is a favorable isotherm. We have measured the isotherm with the three model proteins. The isotherms are shown in Fig. 1. For all proteins very favorable isotherms were obtained.

When superimposed, BTCs of the model proteins obtained on CIM-disks were almost identical. The BTCs are shown in Figs. 2–4. The sole exception was BSA at a concentration of 0.1 mg/mL. From previous

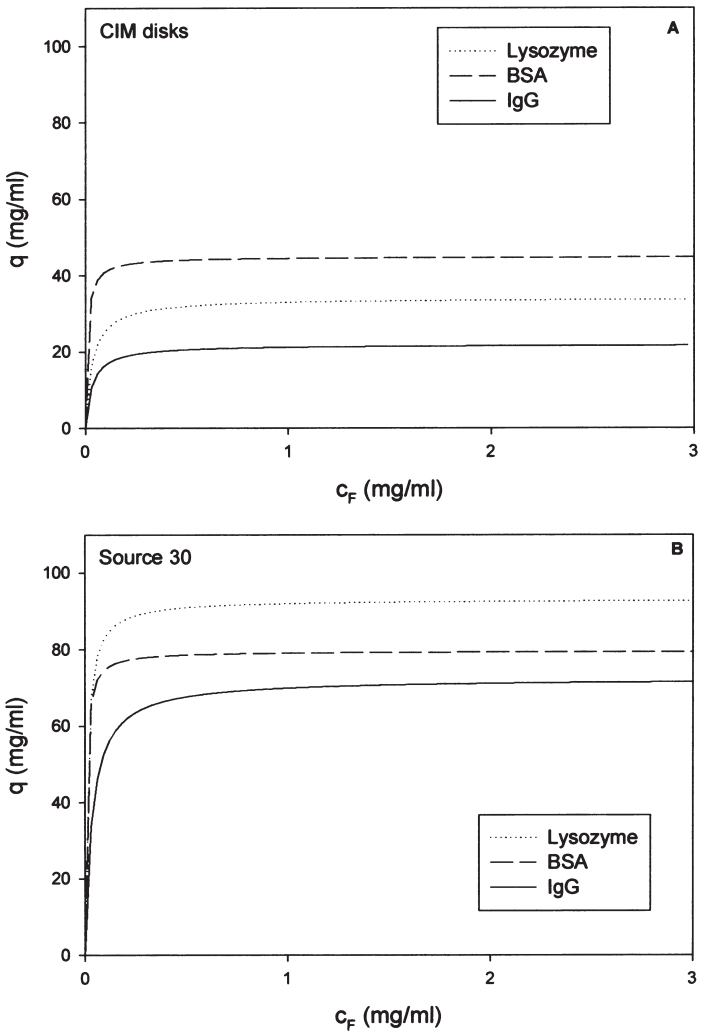

Figure 1. Adsorption isotherm of human IgG, BSA, and lysozyme on A) CIM-disks and B) Source 30.

experiments, we know that it is difficult to regenerate the DEAE disk when loaded with the sticky BSA molecule. At a concentration of 3 mg/mL the BTCs match nicely. Here it can already be seen that the band spreading is caused from axial dispersion caused by nonideality of flow. It seems that there is no significant contribution to the band spreading due to diffusion. In

the case of the particulate material the situation is different. The slope of the BTC depends on the velocity and the feed concentration (Figs. 2–4). Under the applied conditions, it was not possible to develop a full breakthrough although the applied protein exceeded the static capacity. The mass transfer

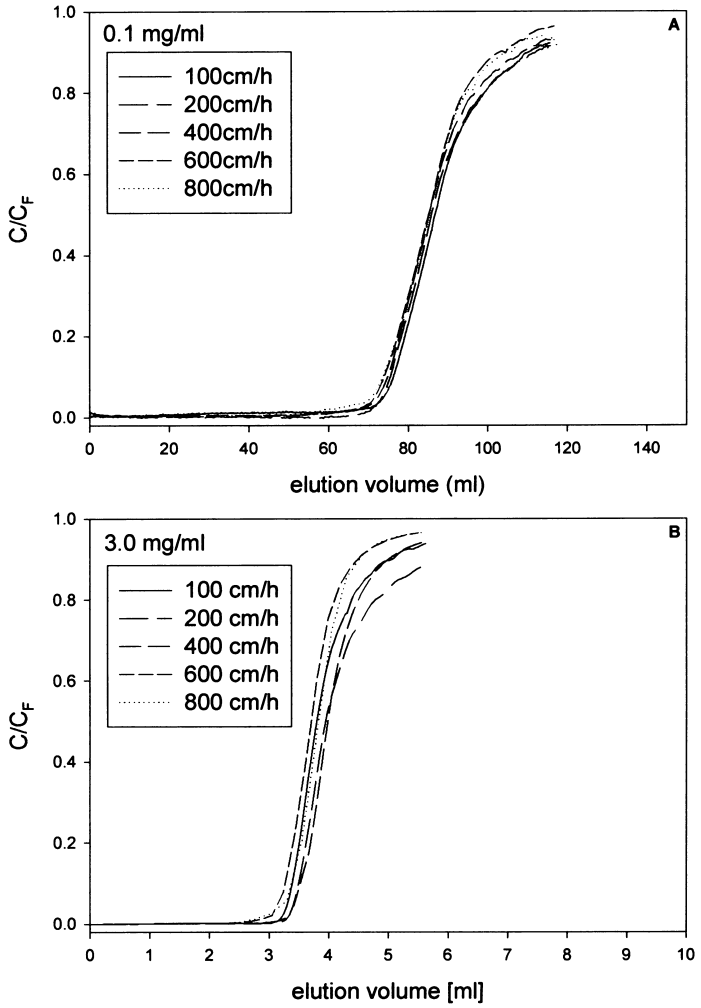

Figure 2. Representative BTCs of lysozyme on CIM-SO_3 and Source 30 S at various velocities and feed concentrations. A) CIM-SO_3, 0.1 mg/mL lysozyme; B) CIM-SO_3, 3.0 mg/mL lysozyme; C) Source 30 S, 0.1 mg/mL lysozyme; and D) Source 30 S, 3.0 mg/mL lysozyme.

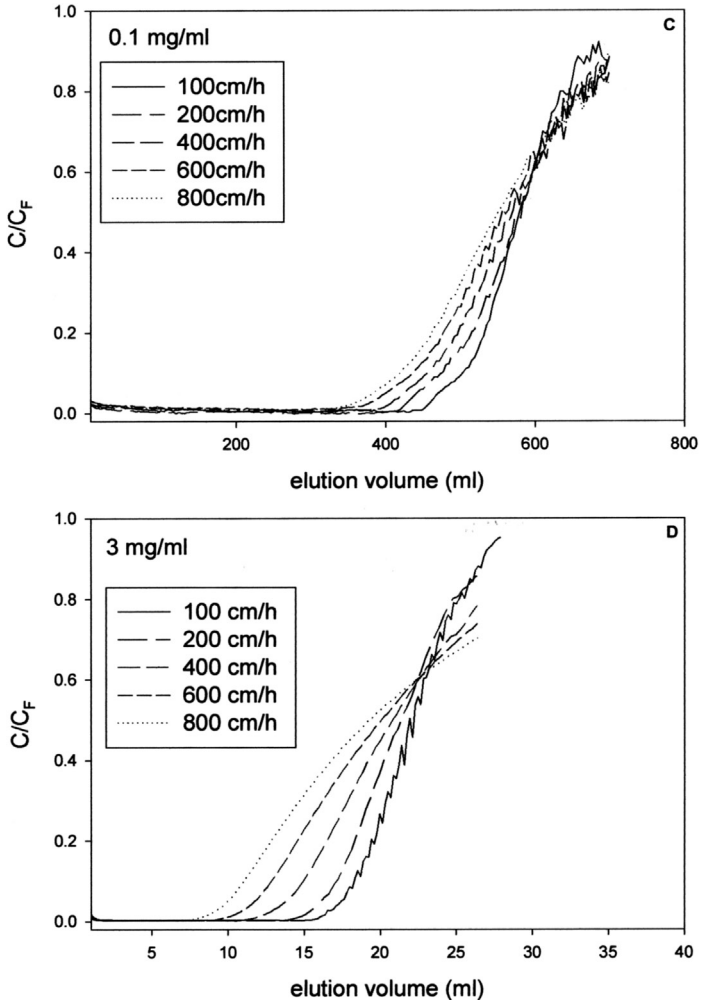

Figure 2. Continued.

zone (MTZ) was extracted for each protein and plotted vs. the normalized feed concentration (Fig. 5). For the monoliths, the width of the MTZ in mg-units is independent of the flow velocity and the protein concentration for a particular protein. This indicates that there is no significant contribution to band spreading due to mass transfer resistances. At high feed concentration the accuracy of the determined BTCs and consequently the MTZ is lower due

to fast breakthrough. Therefore at this concentration the data are more scattered compared to the small concentration range.

From the BTCs at 0.1 mg/mL the HETP values were calculated according to Lettner et al. (18). The curves were approximated with a

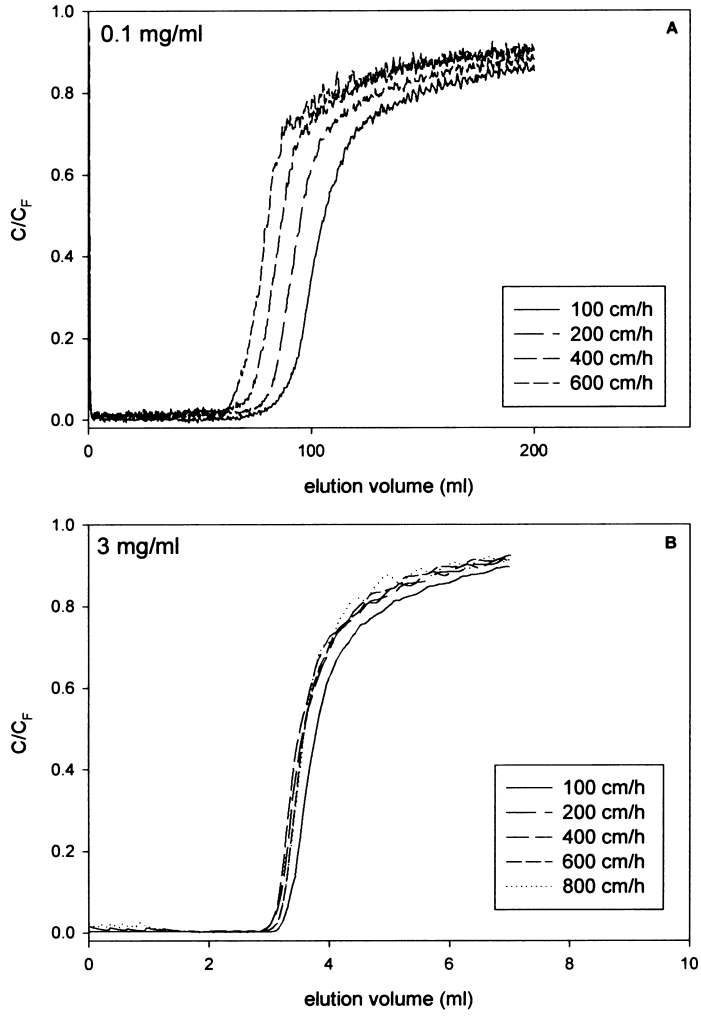

Figure 3. Representative BTCs of BSA on CIM-DEAE and Source 30 Q at various velocities and feed concentrations. A) CIM-DEAE, 0.1 mg/mL BSA; B) CIM-DEAE, 3.0 mg/mL BSA; C) Source 30 Q, 0.1 mg/mL BSA; and D) Source 30 Q, 3.0 mg/mL BSA.

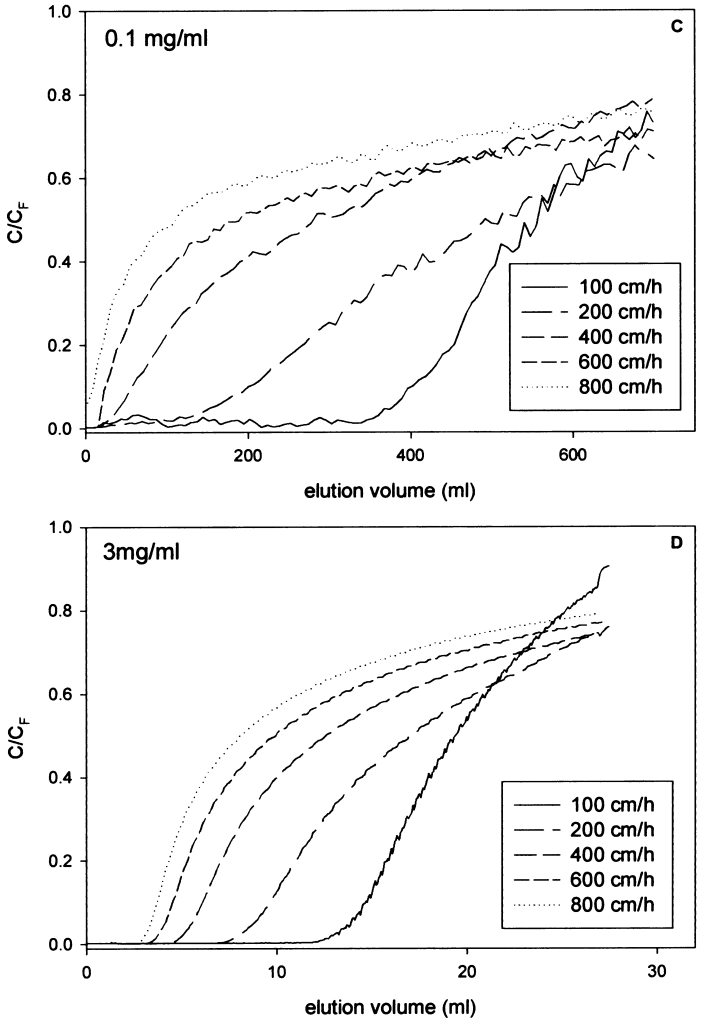

Figure 3. Continued.

cumulative exponential-modified gauss function and the first and the second moment were calculated. The reduced HETP values were plotted against the reduced velocity (Fig. 6). The diffusivity of the proteins were determined according to their molecular mass as described by Tyn and Gusek (19). The monolithic column exhibits a performance independent of the reduced

velocity and protein. The reduced HETP values are in the range of 20. We used a value of 1 μm for the particle size. This value was estimated from scanning electron micrographs (4). It is not clear if the effective particle size in monolithic columns is that low. Knowing the effective particle diameter

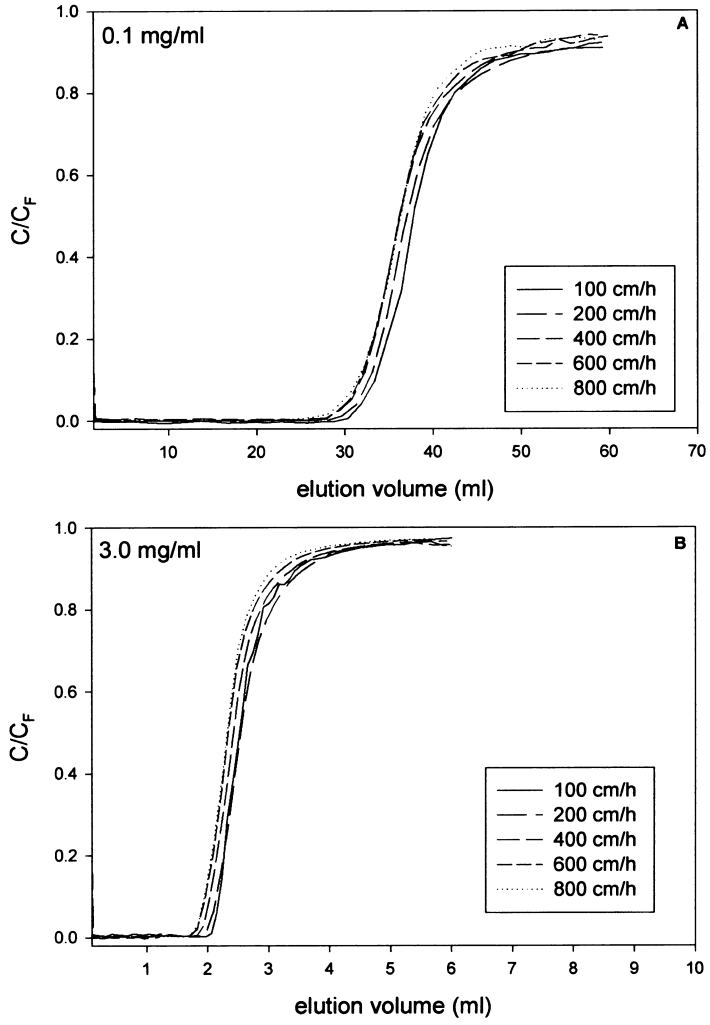

Figure 4. Representative BTCs of IgG on CIM-SO_3 and Source 30 S at various velocities and feed concentrations. A) CIM-SO_3, 0.1 mg/mL IgG; B) CIM-SO_3, 3.0 mg/mL IgG; C) Source 30 S, 0.1 mg/mL IgG; and D) Source 30 S, 3.0 mg/mL IgG.

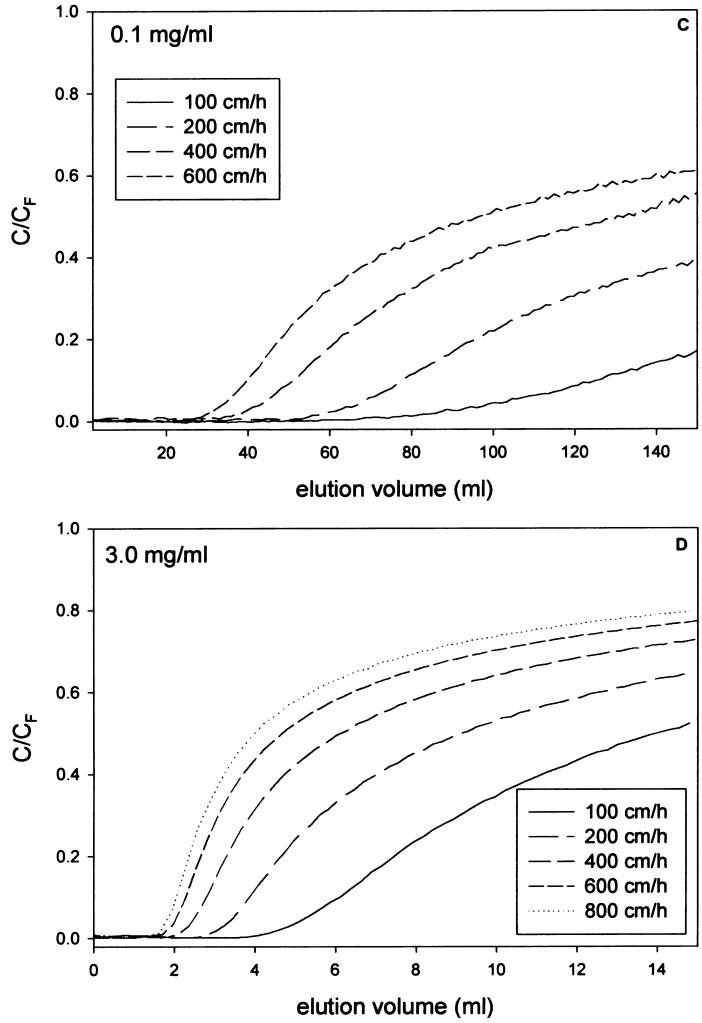

Figure 4. Continued.

would shift the data to a different HETP range. The contribution of the external band spreading was also assessed by BTCs through empty columns when the adaptors have been put together. From BTCs of lysozyme the second peak moments were calculated (Table 1). For the monoliths and the

particulate material the contribution is below 1%. This effect also could not explain the high HETP values. Nevertheless, the important observation is the independence of HETP on the reduced velocity, while the particulate material strongly depends on the reduced velocity.

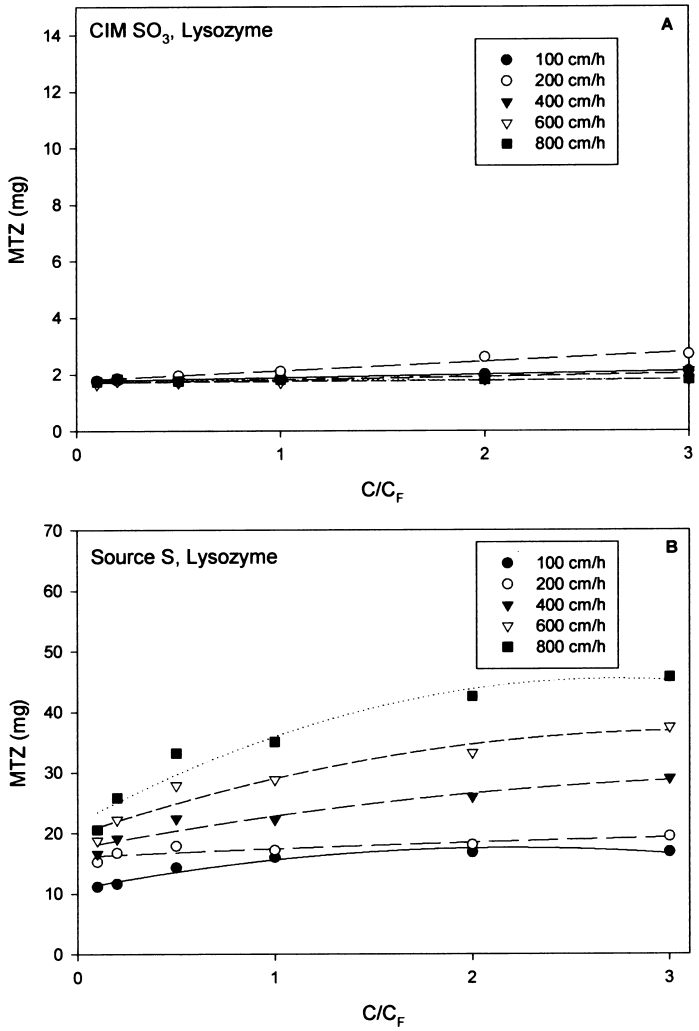

Figure 5. Width of the MTZ in mg depending on feed concentration and flow velocity. A) CIM SO_3, lysozyme; B) Source 30 S, lysozyme; C) CIM DEAE, BSA; D) Source Q, BSA; E) CIM SO_3 IgG; and F) Source S, IgG.

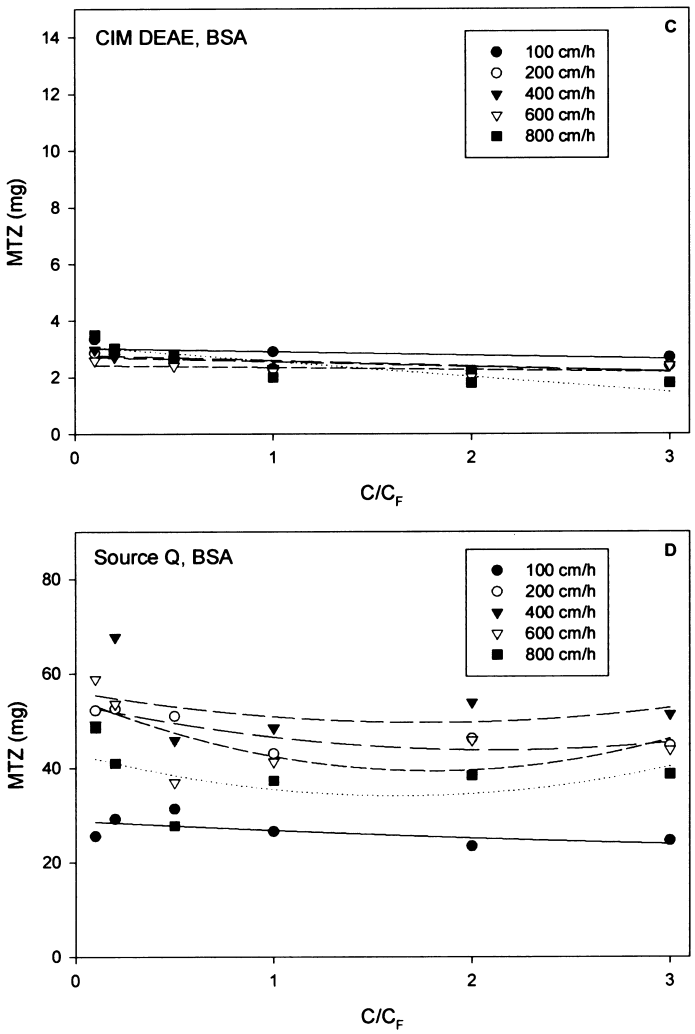

Figure 5. Continued.

(*continued*)

Mass transfer coefficients were only calculated for the particulate material. In the other cases, the two-film model does not apply. The flux was plotted against the normalized feed concentration and the data were approximated by Eq. (11). These graphs are shown in Fig. 7A–C. Data of high velocities (600 and 800 cm/hr) and high feed concentrations (2 and

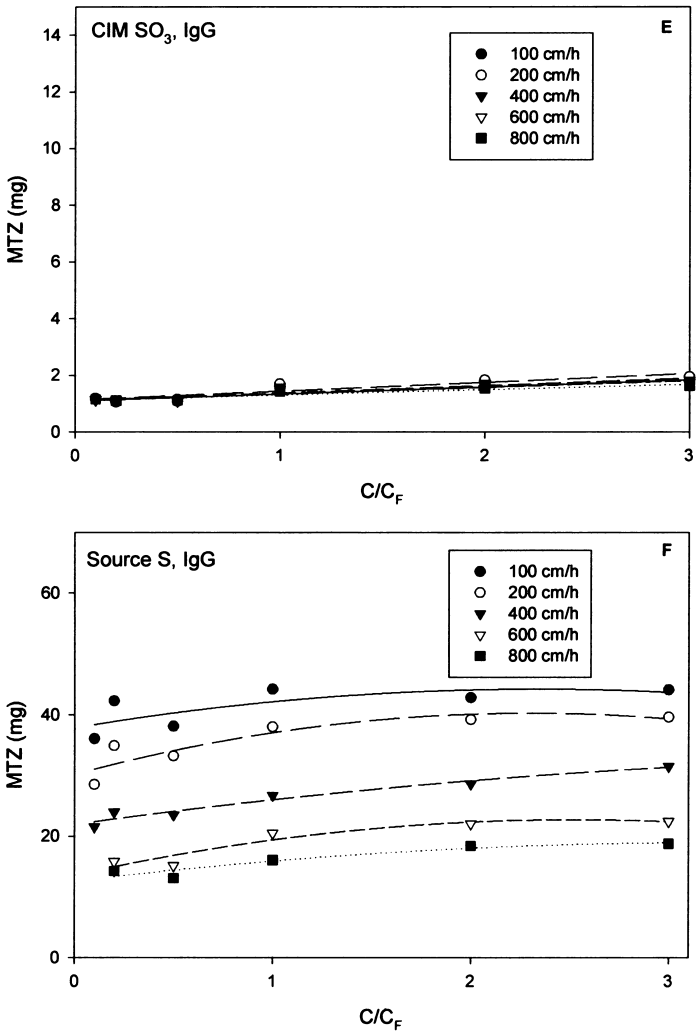

Figure 5. Continued.

3 mg/mL) were approximated by the model assuming particle resistance using Eq. (8). It was refrained to calculate these coefficients for BSA and IgG, since the BTCs were not fully developed. For lysozyme a value of $k_s = 6 \times 10^{-6}$ cm/sec was obtained. The scaled mass transfer resistance δ was in the range of 0.9–10 indicating that both resistances are important. At higher

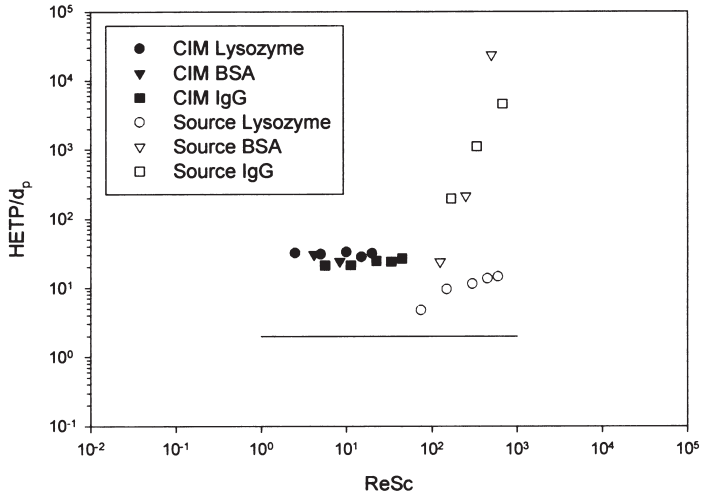

Figure 6. Generalized van Deemter plot: Reduced HETP data calculated from BTCs versus reduced velocity. The line in the lower region represents the theoretical value of 2 assumed for axial dispersion.

concentrations and velocities particle resistance is the dominating resistance. The low k_s value and the relatively high values of δ were not expected and are in contrast to findings of other authors (14,15). A possible explanation is the flat column geometry, which was chosen to elaborate the different mass transfer properties of the two investigated media.

The applied experiments provide an overview of the mass transfer properties of monoliths intended for use in preparative chromatography

Table 1. Second Peak Moments (μ_2) Calculated from Breakthrough Curves with 0.1 mg/mL Lysozyme on Convective Interaction Media Disks and an Empty Cartridge; and on Source and an Empty Column

Velocity (cm/hr)	CIM μ_2 (mL^2)	Empty Cartridge μ_2 (mL^2)	Source μ_2 (mL^2)	Empty Column μ_2 (mL^2)
100	77.6	0.104	3121.9	0.024
200	72.6	0.056	6207.4	0.018
400	77.8		7021.1	
600	65.9		8080.9	
800	74.3		8272.7	

compared to a standard preparative chromatography medium. The most striking observation is that the MTZ is unaffected by the flow rate in monoliths. The equilibrium binding capacity of the particulate medium is at least two times higher compared to the monoliths. The applied model does

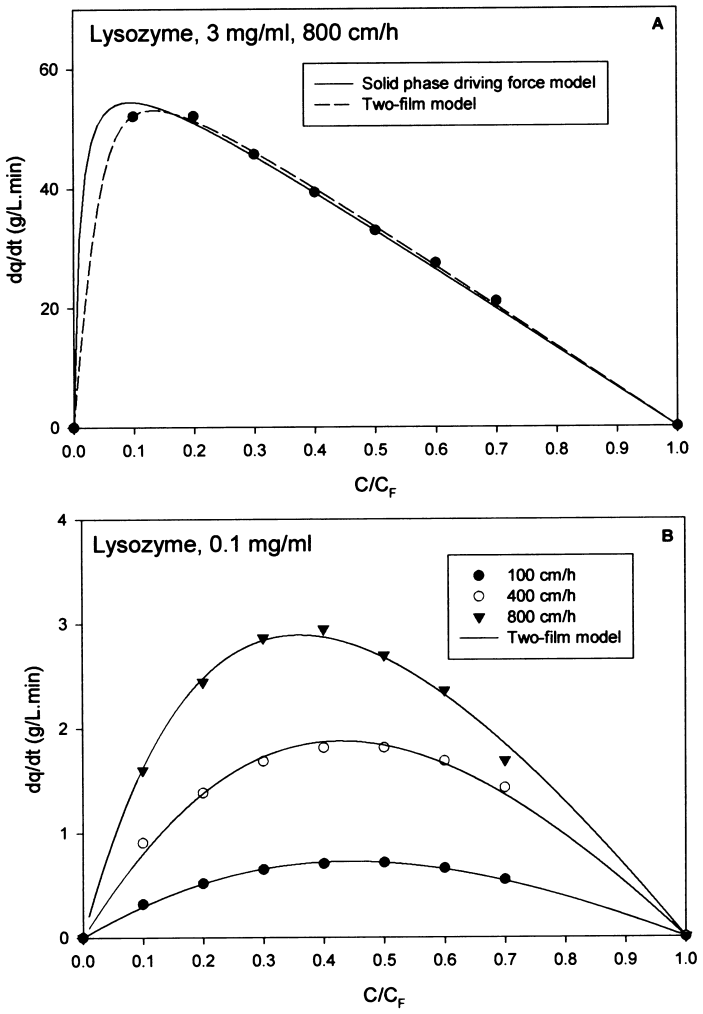

Figure 7. Approximation of experimental flux profiles of lysozyme on Source S with the linear driving force models. A) 3 mg/mL at 800 cm/hr; B) 0.1 mg/mL at 100, 400, and 800 cm/hr; and C) 1.0 mg/mL at 100, 400, and 800 cm/hr.

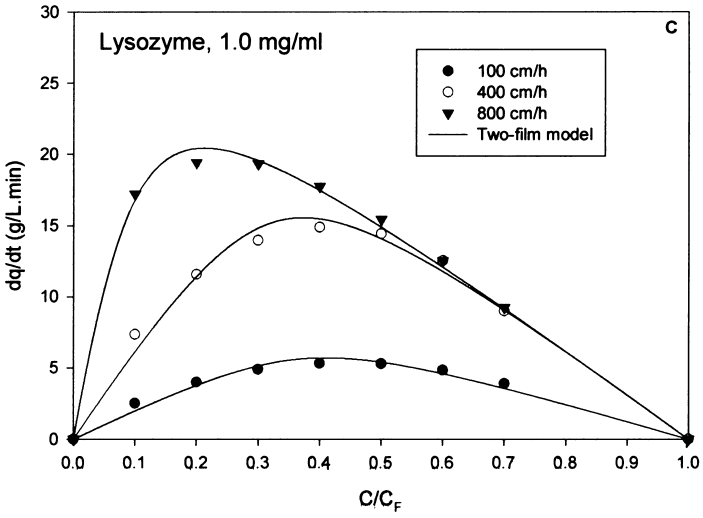

Figure 7. Continued.

not allow one to discriminate between convection and diffusion. One question that remains open is whether the excellent mass transfer properties of monoliths are obtained by enhanced convective transport or just by the small particle size.

SYMBOLS

b	Langmuir parameter
c	mobile phase concentration
c_0	mobile phase concentration at the interphase
c_F	feed concentration
d_p	particle diameter
k_f	external film mass transfer coefficient
k_s	solid phase mass transfer coefficient
q	solid phase concentration
q_0	solid phase concentration at the interphase
q_F	equilibrium feed concentration in particle
u	interstitial mobile phase concentration
x	reduced mobile phase concentration, c/c_F
x_0	reduced mobile phase concentration at the interface, c/c_F
y	reduced solid phase concentration, q/q_F

Greek Letters

β	parameter, bc_F
δ	scaled mass transfer resistance ratio, $k_f c_F / k_s q_F$

ACKNOWLEDGMENTS

The work has been supported in part by the EUREKA project FAST 1 and a grant from the Austrian Research Foundation and OCTAPHARMA, Vienna. We want to thank Amersham Pharmacia Biotech, Uppsala, Sweden and BIA Separations Ljubljana, Slovenia for providing the chromatography material.

REFERENCES

1. Hjerten, S.; Liao, J.L. High-Performance Liquid Chromatography of Proteins on Compressed, Non-porous Agarose Beads. I. Hydrophobic-Interaction Chromatography. J. Chromatogr. **1988**, *457*, 165–174.
2. Tennikova, T.; Svec, F.; Belenkii, B.G. High Performance Membrane Chromatography. A Novel Method of Protein Separation. J. Liq. Chromatogr. **1990**, *13*, 63–70.
3. Minakuchi, H.; Nakanishi, K.; Soga, N.; Ishizuka, N.; Tanaka, N. Octadecylsilylated Porous Silica Rods as Separation Media for Reversed Phase Liquid Chromatography. Anal. Chem. **1996**, *68*, 3498–3501.
4. Hahn, R.; Jungbauer, A. Peak Broadening in Protein Chromatography with Monoliths at Very Fast Separations. Anal. Chem. **2000**, *72*, 4853–4858.
5. Liao, J.L. Continuous Bed for Conventional Column and Capillary Column Chromatography. In *Advances in Chromatography*; Brown, P.R., Grushka, E., Eds.; Marcel Dekker: New York, 2000; 467–502.
6. Tanaka, N.; Nagayama, H.; Kobayashi, H.; Ikegami, T.; Hosoya, K.; Ishizuka, N.; Minakuchi, H.; Nakanishi, K.; Cabrera, K.; Lubda, D. Monolithic Silica Columns for HPLC, Micro-HPLC, and CEC. J. High Resol. Chromatogr. **2000**, *23*, 111–116.
7. Nakanishi, K.; Shikata, H.; Ishizuka, N.; Koheiya, N.; Soga, N. Tailoring Mesopores in Monolithic Macroporous Silica for HPLC. J. High Resol. Chromatogr. **2000**, *23*, 106–110.
8. Josic, D.; Strancar, A. Application of Membranes and Compact Porous Units for Separation of Biopolymers. Ind. Eng. Chem. Res. **1999**, *38*, 333–342.
9. Josic, D.; Buchacher, A.; Jungbauer, A. Monoliths as Stationary Phases for Separation of Proteins and Polynucleotides and Enzymatic Conversion. J. Chromatogr. B **2001**, *752*, 191–205.

10. Meyers, J.J.; Liapis, A.I. Network Modeling of the Convective Flow and Diffusion of Molecules Adsorbing in Monoliths and in Porous Particles Packed in a Chromatographic Column. J. Chromatogr. A **1999**, *852*, 3–23.
11. Iberer, G.; Hahn, R.; Jungbauer, A. Monoliths as Stationary Phases for Separating Biopolymers. LC-GC **1999**, *17*, 998–1005.
12. Garke, G.; Radtschenko, I.; Anspach, F.B. Continuous-Bed Chromatography for the Analysis and Purification of Recombinant Human Basic Fibroblast Growth Factor. J. Chromatogr. A **1999**, *857*, 127–144.
13. Yoshida, H.; Kataoka, T.; Ruthven, D.M. Analytical Solution of the Breakthrough Curve for Rectangular Isotherm System. Chem. Eng. Sci. **1984**, *39*, 1489–1497.
14. Fernandez, M.A.; W., S.; L.; Carta, G. Characterization of Protein Adsorption by Composite Silica–Polyacrylamide Gel Anion Exchangers II. Mass Transfer in Packed Columns and Predictability of Breakthrough Behavior. J. Chromatogr. A **1996**, *746*, 185–198.
15. Hansen, E.; Mollerup, J. Application of the Two-Film Theory to the Determination of Mass Transfer Coefficients for Bovine Serum Albumin on Anion-Exchange Columns. J. Chromatogr. A **1998**, *827*, 259–267.
16. Vermeulen, T. Theory for Irreversible and Constant Pattern Solid Diffusion. Ind. Eng. Chem. **1953**, *45*, 1664–1670.
17. Strancar, A.; Barut, M.; Podgornik, A.; Koselj, P.; Schwinn, H.; Raspor, P.; Josic, D. Application of Compact Porous Tubes for Preparative Isolation of Clotting Factor VIII from Human Plasma. J. Chromatogr. A **1997**, *760*, 117–123.
18. Lettner, H.P.; Kaltenbrunner, O.; Jungbauer, A. HETP in Process Ion-Exchange Chromatography. J. Chromatogr. Sci. **1995**, *33*, 451–457.
19. Tyn, M.T.; Gusek, T.W. Prediction of Diffusion Coefficients of Proteins. Biotechnol. Bioeng. **1990**, *35*, 327–338.